Labial teeth and gingiva color image segmentation for gingival health-state assessment

Timo Eckhard, Eva M. Valero and Juan L. Nieves; University of Granada, Faculty of Science, Optics Department; Granada, Spain

Abstract

Gingival health state assessment has always been considered of great importance in the field of dentistry. A major concern in this area is the subjectivity that commonly applied assessment methods inherit. Most of the previous approaches that aim at introducing objectivity in the assessment are based on data from photographic images of the gingival area. Nevertheless, they generally lack applicability in the clinical environment because of the requirement of expertise in image processing to perform the analysis. In this work, an enhanced teeth region segmentation scheme is proposed, based on the Self-Organizing Map algorithm. The segmentation task is the basis for further objective assessment of gingival health that can entirely be performed automatically. By introducing a novel training image selection approach, the segmentation performance of this task was increased significantly, compared to previous work. Apart from that, a newly developed spatial segmentation feature in addition to color is investigated and evaluated. The novel Labial Teeth and Gingiva Image Database *of the University of Granada is used as benchmark for the segmentation scheme.*

Introduction

A subdivision of oral health care is gingival health state assessment. This research field is mainly devoted to the evaluation of gingival health (ideally in an objective fashion) and the monitoring and/or analysis of a wide range of oral cavity diseases affecting the gingivae. A very prominent amongst these diseases is gingivitis, a form of periodontal disease which involves inflammation and infection of the tissue that supports the teeth. Early detection and treatment are especially important in order to avoid gingivitis advancing to periodontitis and eventually leading to teeth loss [1].

Research in the field of dentistry related to an objective quantification of gingival inflammation dates back to at least the late 1960s [2]. The severity of gingival inflammation is historically assessed by dentists by assigning a score to certain regions of gingivae that aims in quantifying several visual signs of inflammation, such as redness, swelling of gingivae, or bleeding upon probing [1, 3, 4]. A main drawback with such approaches is the strong subjective influence that results from visual assessment or the manual probing process [5, 6, 7, 8, 9, 10]. With the beginning of the digital revolution and an increase in computational performance in the past 20 years, several approaches for gingival health state assessment based on digital image analysis were proposed, which aim at obtaining a higher degree of objectivity [7, 8, 9, 11].

Most of the previous work related to teeth or gingival region segmentation from photographic images does not focus on obtaining an automated segmentation as proposed in this article. These studies are more interested in the medical eligibility or usefulness of an objective approach of gingival heath state assessment. For instance Smith et al. [7] investigate the reliability of measurement of changes in gingival redness and swelling on photographic images. Analysis of the images are carried out in a non-automated fashion: visible gingivae is segmented from the images with a thresholding process by means of the graphics editing software Photoshop by Adobe Systems. Other examples are the work by Denissen et al. [9] or that of Mansjur et al. [11], who propose methods of reproducible image acquisition and measurement of color characteristics of gingivae. Also for those studies, non-automated and supervised approaches were selected to segment gingival regions in images, based on standard commercial software tools. Zakian et al. [8] instead propose a method of gingival inflammation assessment based on photographic images that follows a different approach of teeth region segmentation. Their method involves assigning class membership of image pixels according to some least-square distance algorithm to either the teeth or gingiva class. The class properties are extracted for each image manually by selecting a small area of teeth or gingiva respectively and analysing their color properties. Afterwards, edge detection is applied to the binary class-membership image of teeth and gingiva in order to extract the line contour of the gingival margin. Finally, a manual fine-adjustment of the line-contour is performed via a graphical user interface. The necessity of manual fine-adjustment of the segmentation approach is a drawback when it comes to practical aspects, as specially trained personnel would be needed at dentist practice to perform the health state assessment.

In a previous study [12], we presented some preliminary data on the development of an automated method of objective gingival inflammation assessment, based on colored digital still images. According to that method, a specific image acquisition process for labial teeth and gingiva images (further *LTG images*) was used to acquire colored digital still images from a subject. In a second stage, teeth regions were segmented from gingiva regions in the image. The segmentation is based on the Self-Organizing map (further SOM) algorithm, a type of artificial neural network that showed good performance for the teeth region segmentation task in our previous work. The segmented teeth and gingiva region images are the basis for extraction of several parameters of gingival health.

In this article, a novel approach of teeth region segmentation is documented and discussed. The following section (*The SOM approach applied to image segmentation*) includes a detailed description of the fundamentals of the used segmentation approach. Section *Feature space selection* discusses the selection of an additional spatial features for the segmentation task. Section *Training data selection* introduces the training process of the SOM, whereas segmentation performance evaluation is discussed in section *Segmentation perfromance evaluation*. The results of this work are summarized in section *Results*, and the most relevant conclusions are presented in section *Conclusions*.

The SOM approach applied to image segmentation

The SOM algorithm is a type of artificial neural network with the special property of effectively creating spatially organized internal representations of the input space of a set of training samples (the map). It has been studied extensively in the past 30 years and applied to various fields of research [13, 14]. For the case of image segmentation, the input space of the map is spanned by feature vectors, which could be color coordinates of image pixels or any other type of image features. Spatial locations of neurons on the map then correspond to particular domains of input signal patterns, which makes groups of neurons acting as separate decoders for an input signal pattern [13].

In the present context, the SOM algorithm is used for the task of unsupervised image classification/segmentation in a supervised training scheme. The implementation used is based on a function package that implements the SOM algorithm for Matlab®, called the *SOM Toolbox*[14]. It follows a short description on the SOM training process and the proposed approach for images segmentation.

The learning process

A crucial property of the SOM algorithm is that neurons are addressed as topologically related subsets during the training process, and not independently from each other. Such behaviour is described in biophysically inspired networks as a process of lateral interaction and leads to a local relaxation or smoothing effect on the weight vectors of neurons in a neighbourhood and in the long run to a global ordering. The process responsible for lateral interaction is defined by a *neighbourhood* N_c around neuron c and a *learning rate factor* $\alpha(t)$. N_c can be defined as a function of time ($N_c = N_c(t)$), which allows the number of neurons in the neighbourhood of c to decrease over time (see Figure 1) [13, 15]. Heuristic analysis revealed that a large N_c at the beginning of the learning process, while monotonically decreasing N_c over time, is advantageous. It can be concluded that a large N_c at the beginning leads to a rough global ordering of weight vectors m_i, while a finer N_c in later stages improves the spatial resolution of the map [13]. The iterative updating process of neurons during learning is defined as

$$m_i(t+1) = \begin{cases} m_i(t) + \alpha(t)[x(t) - m_i(t)] & \text{if } i \in N_c(t) \\ m_i(t) & \text{if } i \notin N_c(t) \end{cases} \quad (1)$$

with $\alpha(t)$ in range $0 < \alpha(t) < 1$, for which $\alpha \to 0$ when $t \to \text{inf}$.

Initialization of weight vector m_i for neuron i is performed in a random fashion. As shown above, initially unordered vectors will be ordered in the long run, after a reasonable amount of runs.

The learning process of a map is traditionally applied sequentially: input vectors x are presented to the network and weight vectors are updated iteratively. A much faster alternative approach that was followed in this work is batch learning, where the whole set of input vectors is presented to the map one at a time and new weight vectors are weighted averages of the input vectors.

Performing segmentation

A trained map has the feature, that spatial locations of neurons correspond to particular domains of input signal patterns, as mentioned earlier. Consider a sheet-shaped map with a hexagonal local lattice topology as depicted in Figure 1. The SOM defines a mapping from the n-dimensional input space $\Re^n$ to the two-dimensional array of neurons. Let an input vector $x = [\xi_1, \xi_2, ..., \xi_n]^T \in \Re^n$ be connected to all neurons of the map via scalar weights μ_{ij}. The response of the map to the input vector x is located where the distance between x and m_i is least. Formally, this response is defined as the location of the *best-matching neuron* c, which is obtained as $c = \underset{i}{argmin}\{\|x - m_i\|\}$, according to the euclidean norm. In other words, each image pixel is assigned the class label of the particular neuron on the map that is most similar to the image pixel itself. [13, 14, 15]

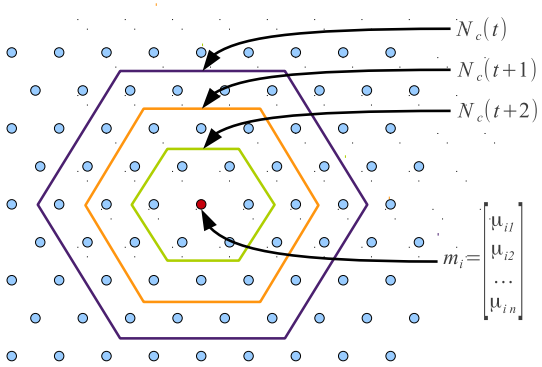

Figure 1. *Illustration of a SOM in sheet shape and hexagonal ordering of neurons. m_i depicts the weight vector of neuron i, the colored hexagons illustrate neighbourhood sets of neuron N_c at different moments in time.*

Feature space selection

The input space of the SOM algorithm can include any type of feature vector. For color image data, the most straight-forward features are color features, namely the color coordinates of image pixels. As the result of an empirical color space selection in previous work, CIE-L*a*b* color space was found to cluster teeth and non-teeth regions in LTG images best and resulted in the lowest segmentation error [16]. Therefore, it was selected for this work as well. Apart from color features, the usage of a novel global spatial feature in addition to color was evaluated. A global spatial feature applies to image content that inherits a strong global spatial relation, as is the case for LTG images: for instance teeth regions are by definition centred vertically and span horizontally over the whole image. Gingival regions on the other hand occupy regions towards the upper and lower border and also span horizontally over the whole image. Taking this a-priori information into account is expected to enhance image segmentation.

Incorporating the a-priori information on global spatial correlation of image content is performed by adding what we call *vote-features* to the images. The vote feature assigns a sort of empirically determined probability for any spatial pixel location in an image as belonging to a certain segmentation class, for instance the *teeth-region* class. Probabilities for pixel locations are calculated from a set of spatially registered sample images, for this work 45 in total. Formally, the vote feature for the teeth region can be described as

$$S_{teeth}(i) = \{w/w = teeth, teeth \in I(i)\} \quad (2)$$

with S_{teeth} being a set of pixels in LTG image $I(i)$, and

$$I_{vote}(x,y) = \sum_{i=1}^{N} \sum_{x=1}^{I(i)_{width}} \sum_{y=1}^{I(i)_{height}} I(i)(x,y) \in S_{teeth} \quad (3)$$

where N denotes the number of all LTG images I used for creation of the vote image I_{vote} and $I(i)(x,y) \in S_{teeth}$ are those pixels in LTG image $I(i)$ which belong to the set of teeth pixels S_{teeth}.

The vote features for each pixel location in an image can be visualized spatially arranged in form of an image, as illustrated in Figure 4 (upper right box, image on the right).

Training data selection

As mentioned earlier, the map of the SOM algorithm is created in an iterative learning process. A main premise of the training process is, that training data is selected as such to represent most closely the data that will be segmented in a later stage. Following such selection, a good generalization of the training process can be achieved, i.e., the classifier is expected to perform well for samples that differ from those of the training set [17]. Commonly applied methods for training data selection are for instance random selection, multiple training or cross-validation [18].

The training data selection for this work is based on a two-stage approach that involves some empirical analysis of a set of available training data. First, from the set of 45 images available for training, those images are selected, that inherit most information amongst the set. The second stage is to condense data samples from the selected images, in order to reduce redundant information and further speed up the training process.

Stage 1: Image selection The image selection task aims at finding such images that inherit the most important information for the training of a map. *Information* in here refers to *color information*, namely the color coordinates of an image pixel in CIE-L*a*b* color space, as this data is used for the classification process. Therefore, in this context the image that inherits most information from a set of images can be defined as the image with the most deviant color coordinates amongst all images, according to some color difference formula. A straight-forward approach would be an iterative comparison of each pixel in an image with any other pixel of all images of the set and accumulating the resulting color differences. However, for the amount of available training samples, this approach is computationally expensive and impractical.

The novel approach proposed in this work is to compare similarities of images according to their color histogram signature. Therefore, similarity between images is computed by comparing the color histograms of the images. The less similar, or the more un-similar an image is, as compared with all other images of a set, the more information is contained and therefore the more suitable it is for training.

A color histogram for an image is a discrete function $h(\vec{r_k}) = n_k$, where r_k is the k-th intensity value and n_k is the number of pixels in the image with intensity r_k [19]. For this work, image histograms are being normalized over the amount of pixels in an image in order to allow comparison of histograms from images of different size. Such normalization is obtained by dividing each component of the histogram by the total amount of pixels in the image. The normalized image histogram is then computed as

$$h(\vec{r_k}) = \frac{n_k}{M * N} \quad (4)$$

with M and N being the image width and height respectively. The cosine similarity between two color histograms $\vec{h_1}$,$\vec{h_2}$ is computed as

$$sim(\vec{h_1}, \vec{h_2}) = \frac{\vec{h_1} * \vec{h_2}}{|\vec{h_1}||\vec{h_2}|} \quad (5)$$

where the numerator represents the dot product of the vectors $\vec{h_1}$ and $\vec{h_2}$ and the denominator being the product of their *Euclidean norm*. A cosine similarity of one refers to an angle of 0 degree between the color histograms of two images and therefore to images that have an equal amount of pixels in each bin of the histogram. A cosine similarity of zero refers to images that are maximally different.
For the case of training image selection, an iteration is performed over the whole set of images. For each candidate image, the cosine similarity between its histogram and the histograms of the remaining images is computed. This approach allows an ordering of similarities of images, based on the sum of cosine similarities S within the set of all images, defined as

$$S(\vec{h_c}) = \sum_{i=1}^{n} sim(\vec{h_c}, \vec{h_i}) \quad (6)$$

with n being the number of histograms in the set, $\vec{h_i}$ the i-th histogram and $\vec{h_c}$ being the candidate histogram for S. A great advantage of this novel approach is, that color- as well as spatial-properties are included in the selection process, as the frequency of occurrence of individual colors is taken into account as well as the occurrence of a color itself (see Figure 2).

Stage 2: Data sample condensation An average sample image from the set of available images for training consists of about half a million pixels. As such images are captured in a rather high resolution, it is expected that they inherit a lot of redundant information. Aiming to minimize the number of pixels selected for the SOM training, a simple random selection is applied for each individual image. For this work, a fraction of 20% randomly selected, equal distributed data points was empirically found to perform well.

Segmentation performance evaluation

Segmentation performance in this context refers solely to the segmentation quality that can be obtained for the given image segmentation task and not to computational complexity or computational performance. The reason for this is that the analysis of images for gingival health state assessment is not necessarily a time-critical process.

Error measure

The performance of image segmentation in terms of segmentation quality is computed as the sum of percentage of pixels of teeth classified wrongly as non-teeth and percentage of

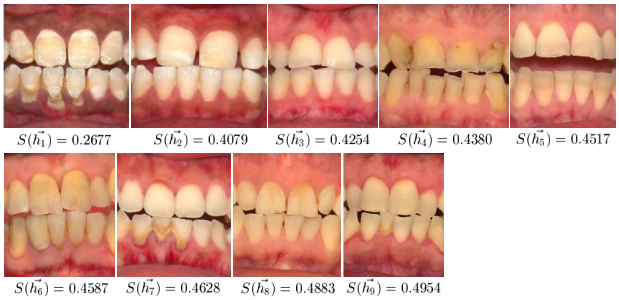

Figure 2. *Optimal training images and corresponding summed cosine similarities: the smaller the summed cosine similarity, the more different the image (in terms of its color histogram signature, compared with the remaining images).*

Table 1: Segmentation error statistics in the feature selection process: μ refers to the mean segmentation error, σ its standard deviation, $95e$ the 95th-percentil and min.error/max.error the images with the minimum and maximum segmentation error respectively

error measure	color	color + init. vote	color + enh. vote
μ (%)	*2.09*	*3.34*	*3.19*
σ (%)	*0.43*	*1.11*	*0.89*
95e (%)	*2.74*	*4.66*	*4.83*
min. error (%)	*1.37*	*1.17*	*1.17*
max. error (%)	*3.49*	*6.49*	*5.26*

pixels of non-teeth classified wrongly as teeth (discrepancy empirical quality measure [20]), compared to manual segmented groundtruth of individual images. The measure can be described formally for the two-class case, for instance for class 1 as

$$E_{c1} = \frac{\sum_{i \in c2} S_{c1}(i)}{\sum_{i \in c1} GT_{c1}(i)} + \frac{\sum_{i \in c1} S_{c2}(i)}{\sum_{i \in c2} GT_{c2}(i)} \quad (7)$$

with S being the class labelled image for class $c1$ and $c2$, and GT its manually class labelled counterpart. $i \in cn$ are the indexes of pixels in an image belonging to class n and the resulting relative error for class $c1$ is depicted as E_{c1}.

Labial Teeth and Gingiva image database

In order to assess the segmentation quality of the SOM approach, a novel image database of LTG images from the University of Granada in Spain was used as benchmark. The initial version of the so called *Labial Teeth and Gingiva Image Database* (further *LTG-IDB*) consists of several GBs of photographic images from 27 subjects with normal oral health. For the task of teeth and non-teeth region segmentation, groundtruth image data, manually segmented from one expert observer, is included. More details on the image database can be found from the technical report at [21].

An important feature of this database is that all images were acquired in a well-defined and documented image acquisition process, optimized for LTG image capturing. Given the static image acquisition parameters, it can be expected that an image segmentation performance evaluation based on this database inherits a high degree of generality for images that are captured in a similar manner, even if they are not included in the database.

Another advantage of using this database is the fact that it is rendered publicly available under a creative common license and can therefore be used by others as well, for instance as benchmark for similar tasks.

Results

Training image selection

The selection of an optimal set of training images was performed on a set of 45 images from the LTG-IDB. The number of optimal training images for the SOM segmentation process was empirically found to be 9. Those images with corresponding summed color histogram similarities are illustrated in Figure 2.

The novel approach of training image selection has the special property of incorporating spatial as well as color information. This behaviour can be illustrated in an artificial example: Figure 3 (upper box left) shows a sample LTG image. In the other images of this box (middle and right), the tooth size was artificially expanded to two different levels respectively, without introducing new colors. The cosine similarity between (left) and (middle) is 0.9492, whereas 0.9184 can be found between (left) and (right). That means that the larger the difference in teeth area in the image, the less similar they are. So the similarity of the color histogram is influenced by the spatial content, in this example the tooth size.

A similar behaviour can be shown for changes that are only applied to the color of the images, while maintaining spatial properties. Figure 3 (lower box) illustrates an example where image saturation was modified in two levels. The cosine similarity between the original image (left) and (middle) is 0.7527, whereas 0.6604 can be found between (left) and (right).

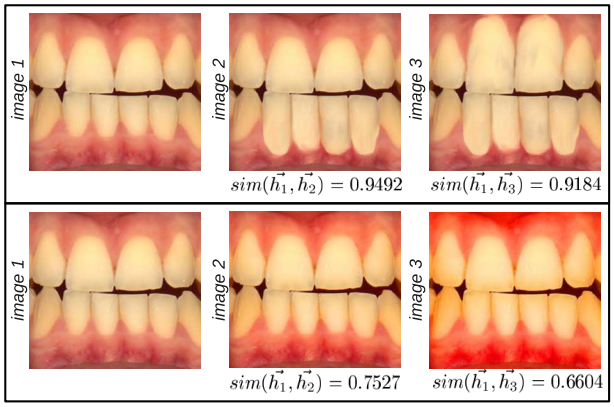

Figure 3. *Upper box: spatial information dependency of color histogram similarity: (left) sample LTG image, (middle) expanded teeth region, (right) further expanded teeth region; Lower box: color information dependency of color histogram similarity: (left) sample LTG image, (middle) slightly increased saturation, (right) heavily increased saturation.*

Feature space selection

Feature space selection was evaluated by performing image segmentation for the whole set of 45 available LTG images from the LTG-IDB, first with color-only features and then with color and an initial version of the vote feature. Also, an enhanced version of the vote feature that is being introduced a bit later, was evaluated. The segmentation error was calculated according to Equation 7 and the map was trained from the optimal training images as described in the previous section.

Column 2 and 3 of Table 1 summarize the segmentation

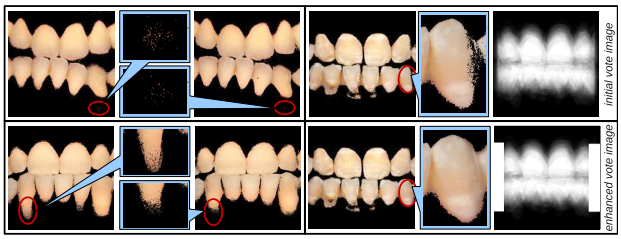

Figure 4. *Examples of assets and drawbacks of color and vote feature selection.*

quality achieved with the two feature set combinations. Apparently, color only features outperformed the color and vote feature combination. This is surprising, as it was expected that the additional information of global spatial correlation of LTG images could enhance image segmentation. However, a closer look on the resulting segmented images gives an insight in the assets and drawbacks of this approach. Figure 4 (upper left box), for instance, illustrates a case where incorporating the spatial feature increases the segmentation performance, compared to using only color features. It can be seen that segmentation based on color-only features (left image) is erroneous for some pixels far apart from the expected location of teeth in an LTG image. The miss-classification is due to the color properties of these pixels, which are close to what is expected to belong to the teeth class but obviously belong to the non-teeth class. Incorporating the spatial feature (right image) restricts most of these pixels to be classified as teeth, as the spatial location of the pixels differs too much from the teeth region location in the vote image (see Figure 4, .

A main drawback from using the spatial feature in its initial version can be observed in Figure 4 (upper right box): a very high rate of miss-classification occurs on the left and right side of most images. The reason for this can be traced back to the design of the vote image. As explained in section *Feature space selection*, votes are collected from sample images for every pixel that belongs to the teeth class. As the size of jaws of individual subjects vary, creating the vote feature as explained earlier leads to a rather fuzzy representation for spatial locations at the horizontal extremes of the images. A way to account for this effect is to modify the vote image in these regions, for instance as illustrated in Figure 4 (lower right box, image on the right). For the illustrated sample image (upper and lower box on the right side, left image) a decrease in segmentation error can be observed when using the modified version of the vote image. Measuring the performance of the whole set of images with the modified vote feature reveals the same results (see Table 1, column 4).

Another observation can be drawn from Figure 4 (lower left box). The tooth shapes of this sample image deviate strongly from the tooth shapes of most other images that were used for creation of the vote feature. This fact leads to a high miss-classification rate for pixels in spatial locations of the image, where the probability for teeth occurrence is small, in accordance to the vote image. It is very likely possible to reduce this kind of error if a larger set of sample images is included in the vote feature creation process. It is expected that by doing so, using color and vote features could outperform the usage of color-only features. We plan to investigate this aspect in future work.

Table 2: Comparison of segmentation error statistics from previous and current results of the teeth segmentation process: μ refers to the mean segmentation error, σ its standard deviation, $95e$ the 95th-percentil and min.error/max.error the images with the minimum and maximum segmentation error respectively

	previous result	current result
μ (%)	5.09	2.09
σ (%)	0.94	0.43
95e (%)	6.66	2.74
min. error (%)	3.20	1.37
max. error (%)	7.38	3.49

Enhancement in segmentation quality for the teeth region segmentation from previous results

In our previous studies [12], the SOM algorithm was used in standard configuration as provided by the SOM Tooolbox. That means that the map was constructed in rectangular map lattice and no post-processing applied to the SOM segmented images. Apart from that, training images were selected in a random fashion for the set of 45 sample images of the LTG-IDB. Following this approach resulted in a mean segmentation error of 5.09% with the 95th-percentil of 6.66% (see Table 2, left column). For this work, using the optimal set of training images and a map built using hexagonal map lattice with a simple binary close post-processing operation on the binary class label image after segmentation could improve the results of the segmentation process impressively. The remaining segmentation error is found to be 2.09% with the 95th-percentil of 1.35% (see Table 2, right column).

It is worth discussing if it proves useful to try to decrease the remaining mean segmentation error further by modifying training process, feature space selection or the SOM algorithm parameters, or if main changes on the design of the experiment are required. Such changes could for instance be capturing new LTG image data or obtaining additional groundtruth information.

Capturing new LTG image data would be an important step in order to assess the generality of the segmentation performance, for a data set with an (expected) larger variability. Obtaining additional groundtruth information on the other hand is a critical step that should be considered in any case. It has been mentioned earlier that the segmentation error is quantified as compared to manually segmented groundtruth data. The manual segmentation for the currently available data set of 45 LTG images has been performed by one expert observer only, namely the first author of this work. An underlying subjectivity is therefore certain, which makes quite doubtful that enhancing the segmentation further is really possible. The remaining approximately 2% mean segmentation error might well be near the uncertainty threshold of the groundtruth data, due to subjectivity. If that is the case, a further enhancement could not be measured based on the available groundtruth data. One way to escape this limitation would be to collect more opinions on groundtruth segmentation for the current data set from other observers and to compare them on a statistical basis, forming a *mean groundtruth*. Following such approach could lead to a more general solution for the groundtruth data and also allow to estimate a groundtruth uncertainty, which would be the inter-observer variance. This aspect shall be treated in future work.

Conclusions

In this work, teeth-region segmentation, a particularly important problem in the process of creating an automated and objective method of gingival health-state assessment, is discussed. The image segmentation task is performed in an unsupervised fashion with supervised training, based on the SOM algorithm. A novel training image selection method is proposed, which aims at quantifying spatial and color differences in image content, based on a color image histogram similarity criterion. According to the optimal training image selection from maximally different images, a map with a high degree of generality could be obtained. Usage of this map led to an increase in performance for the teeth region segmentation process of more than 50%. The training image selection and image segmentation performance were evaluated with images from the LTG-IDB, a novel database of images of labial teeth and gingiva, created and rendered publicly available by the University of Granada. Apart from proposing the novel training image selection scheme, incorporating a global spatial feature in addition to color features in the segmentation process is evaluated. The so-called vote feature takes into account a-priori information on the spatial distribution of image content for segmentation. The performance of using spatial and color features versus color features is evaluated by quantifying the resulting segmentation error. It was found that color features outperform color and spatial features in the current set-up. However, the authors believe that this might be due to the fact that the vote feature lacks some generality, as the set of images used for extraction of the latter is only 45. It is expected, that vote and color feature can outperform color only features, if a larger number of images for creation of this feature would be available.

Finally, the performance of the optimized segmentation approach as presented in this work is compared with previous results for the same segmentation task. The previous mean segmentation error of 5.09% for the teeth segmentation task could be enhanced further to a remaining error of 2.09%, which is believed to be close to what is expected to be the residual error in the groundtruth image data that was used for performance evaluation.

References

[1] R.C. Page, Gingivitis*, Journal of Clinical Peridontology, 13(5), 345-355 (1986)

[2] H. Loe, E. Theilade, S.B. Jensen, C.R. Schitt, Experimental gingivitis in man, Journal of Peridontal Research, 2(4),282-289 (1967)

[3] American Academy of Periodontology, Parameter on plaque-induced gingivitis, Journal of Peridontology 71(5), 851-2, (2000)

[4] G.C. Armitage, The complete peridontal examination, Peridontology 2004, 34(1),22-33,(2004)

[5] R.R. Lobene, Discussion: Current status of indices for measuring gingivitis, Journal of Clinical Peridontology, 13(5),381-382,(1986)

[6] M. Ilyama, K. Saito, H. Horiuchi, H. Shimauchi, R.I. Marshall, P.M. Bartold, Applicability of a computer assisted system for the evaluation of gingival status in subjects from Asian and Caucasian backgrounds, Journal of the International Academy of Peridontology, 41,26-32, (2002)

[7] R. Smith, D. Lath, A. Rawlinson, M. Karmo, a. Brook, Gingival inflammation assessment by image analysis: measurement and validation, International Journal of Dental Hygiene, 682),137-142, (2008)

[8] C. Zakian, I. Pretty, R. Ellwood, D. Hamlin, In vivo quantification of gingival inflammation using spectral imaging, Journal of Biomedical optics, 13, (2008)

[9] H. Denissen, A. Kuijkens, A. Dozi, A photographic method to measure the colour characteristics of healthy gingiva, International Journal of Dental Hygiene, 5(1), 22-26, (2007)

[10] J.S. Ellis, R.A. Seymour, P. Robertson, T.J. Butler, J.M. Thomason, Photographic scoring of gingival overgrowth, Journal of Clinical Periodontology, 28(1),81-85,(2001)

[11] N. Mansjur, U. Masatoshi, T. Takayoshi, O. Chizuko, S. Takeo, M. Yoshimasa, T. Yoichiro, I. Hisao, New method using image analysis to measure gingival color, Journal of Osaka Dental Universitz, 38(1),37-40, (2004)

[12] T. Eckhard, E.M. Valero, F. Mesa, Towards an automated method of gingival inflammation assessment on colored digital still images, 2011 Proc. of the International Color Association, 372-376, (2011)

[13] T. Kohonen, The self-organizing map, Proc. of the IEEE, vol. 78,1464-1480, (1990)

[14] J. Vesanto, J. Himberg, E. Alhoniemi, J. Parhankangas, Self-organizing map in Matlab: the SOM Toolbox, Proc. of the Matlab DSP Conference, 35-40, (2000)

[15] T. Kohonen, The Self-Organizing Map, Springer Series in Information Sciences, 1997

[16] T. Eckhard, E.M. Valero, Task-specific color space selection for image segmentation, In 17. Workshop Farbbildverarbeitung (editor M. Schnitzlein, Chromasens GmbH), 51-60, (2011)

[17] C.M. Bishop, Pattern Recognition and Machine Learning (Information Science and Statistics), Springer, (2006)

[18] N. Philip, What is there in a training sample?, Proc. of the Nature Biologically Inspired Computing, 1507-1511, (2009)

[19] R.C. Gonzales, Digital Image Processing, Tom Robbing, 2nd edition, 2002

[20] H. Zhang, J.E. Fritts, S.A. Goldman, Image segmentation evaluation: a survey of unsupervised methods, Computer Vision and Image Understanding, 110(2), 260-280, 2008

[21] Reading from the web: colorimg homepage of the University of Granada: http://www.ugre.es/local/colorimg, visited Oct. 2011, (2011)

Author Biography

Timo Eckhard received a multiple M.Sc. degree in 2011, awarded by the University of Granada (Spain), the University of Eastern Finland (Finland), the University College Gjøvik (Norway) and the University of Saint-Étienne (France) within the framework of the International Erasmus Mundus Master Program CIMET (Color in Informatics and Media Technology). Timo is currently a Ph.D. student and member of the Color Imaging Lab at the Optics Department of the University of Granada. His research affiliations are Multispectral Science, Color Science and Image Processing.

Eva M. Valero obtained a B.D. in Physics in 1995, and a Ph.D. in 2000, both at the University of Granada. She has worked at the Department of Optics as Associate Prof. since 2001. Shes a member of the Color Imaging Lab at the University of Granada. Her research interests were initially spatial color vision, and more recently multispectral imaging and color image processing.

Juan Luis Nieves received his M.Sc. and Ph.D. in Physics from University of Granada, Granada, Spain, in 1991 and 1996, respectively. He is currently an associate professor at the Department of Optics in the Science Faculty, University of Granada. At present his research in the Color Imaging Lab at the Department of Optics revolves around computational color vision (color constancy, human visual system processing of spatio-chromatic information), and spectral analysis of color images.